6. ANKARA INTERNATIONAL AEROSPACE CONFERENCE AIAC-2011-092
14-16 September 2011 - METU, Ankara TURKEY

REVERSE ENGINEERING OF A MICRO TURBOJET ENGINE

Onur Tuncer* and Ramiz Ömür İçke†
Istanbul Technical University
Istanbul, Turkey

ABSTRACT

Reverse engineering is the process of discovering the technological working principles of a device, object or system. This paper in particular, focuses on the reverse engineering of a micro turbojet engine. First, components of gas turbine geometry are scanned and transformed into digitized point cloud format utilizing a three axis scanner. Next, solid geometry of the engine parts were re-constructed in computer aided drafting environment from these data. Furthermore, performance maps of individual components are either calculated or certain assumptions were made as to their behaviour. On and off design point engine performance has been determined through a parametric cycle analysis. Obtained results are in line with the reported performance parameters of the reverse engineered engine. This study demonstrates the use of reverse engineering procedures, when designing from scratch would not be as practical. This approach can cut down the overall turnover time for a new design.

NOMENCLATURE

a_0	Sonic velocity $[m/s]$
A_9	Nozzle exit area $[m^2]$
c_{p_c}	Heat capacity at the cold section $[J/(kgK)]$
c_{p_t}	Heat capacity at the hot section $[J/(kgK)]$
e_c	Polytropic efficiency of the compressor
e_t	Polytropic efficiency of the turbine
f	Fuel/air ratio
F	Engine thrust $[N]$
h_{PR}	Combustion enthalpy $[J/kg]$
$h_{t_{be}}$	enthalpy of the total burner exit $[J/kg]$
h_0	Enthalpy of the ambient air $[J/kg]$
h_{t1}	Total enthalpy at the compressor inlet $[J/kg]$
h_{t3}	Total enthalpy at the compressor exit $[J/kg]$
$\dot{m}_f$	Fuel mass flow rate $[kg/s]$
$\dot{m}_0$	Air mass flow rate $[kg/s]$
M_0	Mach number at the inlet
M_9	Mach number at the nozzle exit
n	Number of vanes of the centrifugal compressor
P_{t1}	Total pressure value at the inlet $[kPa]$
P_0	Atmospheric pressure $[kPa]$
P_{t2}	Total pressure at the compressor inlet$[kPa]$

*Assist. Prof. in Dept. of Aeronautical Engineering, Email: tuncero@itu.edu.tr
†Graduate Student in Dept. of Aeronautical Engineering, Email:icker@itu.edu.tr

P_{t3} Total pressure at the compressor exit $[kPa]$
P_{t4} Total pressure at the turbine inlet $[kPa]$
P_{t5} Total pressure at the turbine exit $[kPa]$
P_{t9} Total pressure at the nozzle exit $[kPa]$
P_9 Static pressure at the nozzle exit $[kPa]$
r Compressor mean radius $[m]$
R_c Gas constant at the cold section $[J/(kgK)]$
R_t Gas constant at the hot region $[J/(kgK)]$
S Thrust specific fuel consumption $[J/(kgK)]$
T_0 Atmospheric temperature $[K]$
T_{t1} Total temperature value at the compressor inlet $[K]$
T_{t3} Total temperature value at the compressor exit $[K]$
T_{t4} Total temperature at the turbine inlet $[K]$
U_t Tangential velocity $[m/s]$
V_0 Freestream velocity $[m/s]$
v_2 Swirl velocity $[m/s]$
$\dot{w}_c$ Rate of work done by the compressor $[J/kg]$
γ_c Specific heat ratio for the cold section
γ_t Specific heat ratio at the hot section
ϵ Slip factor
η_b Burner efficiency
η_r Recovery efficiency
η_c Compressor isentropic efficiency
η_o Overall efficiency
η_t Turbine efficiency
η_T Thermal efficiency
η_P Propulsive efficiency
π_c Compressor total pressure ratio
π_t Turbine total pressure ratio
π_r Total pressure recovery ratio
π_d Diffuser total pressure ratio
π_n Nozzle total pressure ratio
τ_c Total temperature ratio across the compressor
τ_t Total Temperature ratio across turbine
τ_r Recovery total temperature ratio
ω Angular velocity of the rotor $[rad/s]$

INTRODUCTION

A micro turbojet engine is a small scale gas turbine engine, that can be utilized to provide thrust for a micro scale unmanned air vehicle (UAV). Note that micro engine technology is both robust and affordable, and these engines are well suited for applications such as target and surveillance drones[1],[2].

This study aims at designing a micro turbojet engine through a reverse engineering procedure. The engine used in this study (Simjet 2300-S-25 AES-GE) is shown in Figure 1. This engine has a centrifugal compressor, a single stage axial flow turbine, an annular combustion chamber, a bellmouth inlet and a fixed convergent nozzle. It operates on the open Brayton cycle. This engine runs on liquid fuel, either Jet-A or kerosene. It does not require a seperate oil reservoir since the hybrid bearing are lubricated by a small amount of oil added to the fuel. This yields maximum reliability and robustness. The engine utilizes a Full Authority Digital Engine Controller (FADEC) unit with pre-programmed software. This software offers certain features such as; assisted start-up and shut-down programmes, data display, retrieval and storage, exhaust gas temperature (EGT), shaft speed and engine condition etc.

In this study, not only the engine parts are re-constructed in the computer aided drafting (CAD) environment, but also engine performance parameters are recovered through a detailed cycle analysis. Performance metrics such as specific fuel consumption, specific thrust, thermal efficiency and propulsive efficiency, are calculated as an outcome of this cycle analysis.

This reverse engineering approach can significantly cut down the turn over time for a new micro-scale aero-

engine design rather than starting from scratch. Furthermore this design can later on be used as a baseline engine for other prospective studies.

SOLID MODELING

In order to determine the engine components' geometric features, parts of the engine have been disassembled and scanned by a three axis scanner (ATOS HR 3D) which is shown in Figure 2. Optical scanners work on the basis of using structured light. A known pattern of light is projected on the object and a camera records the image of the pattern with the real image of the part. The system composes of two cameras. One of the cameras act as a light source which illuminates the part with a known pattern, while the other camera digitizes the illumination and acquire the image of the part[3]. Note that only parts that have complex geometries are scanned. The other ones that do not have not complex geometries are simply measured by a calliper. The challenge in this task is to transform the point cloud data obtained from the scan into a solid CAD model. Therefore, point cloud models have been transformed into the solid parts. A commercial CAD program is used for both geometric modelling and assembly.

Figure 3 shows the rotor of the single stage axial turbine of the engine. It generates the power consumed by the centrifugal compressor. This part is made of an Inconel alloy for high temperature resistance. Blade profile slightly changes from hub to tip for optimal blade loading and thus efficiency.

Figure 4 shows the impeller of the centrifugal compressor. Centrifugal compressors provide higher pressure ratios than axial compressors. The pressure ratio generated by a centrifugal compressor ranges from 3 to 7 for small gas turbines[4]. For a desired pressure increase, fewer stages can be used in comparison to axial compressors. Furthermore, the operating speed of the centrifugal compressors are higher than other types of compressors. The geometry of the impellers of a centrifugal compressor is simpler with respect to axial compressor impellers. Consequently, manufacturing costs are lower. All in all, for compact systems which require low cost, low stages,large operating ranges and high pressure ratios such as micro turbojet engines centrifugal compressors offer the best choice.

Splitter blades are another important part of impellers. Splitters are placed circumferentially between the main blades. These can be seen in Figure 4. Splitter blades are utilized to improve the overall performance in terms of efficiency and pressure ratio. Splitters reduce the load on the main blades and may introduce additional losses that depend on their geometry [5]. They achieve this by altering the boundary layer structure. Also note that, this particular design employs back-swept blades.

The corresponding diffuser part is shown in Figure 5. This part converts the kinetic energy of the flow into pressure.

Turbine inlet guide vane, which shown in Figure 6 alters the direction of the flow prior to rotor entrance, such that a maximum amount of work can be extracted from it.

Combustion chamber of the engine is shown in Figure 7. As seen in the figure this combustor is an annular one. So there is only one single volume where entire combustion takes place. Annular combustors are advantageous in terms volumetric heat release. Note that typical gas turbine combustors have a volumetric heat release rate of 200-400 MW/m^3 [6]. Since annular combustors save volume they also save weight, which is very important for aeronautical applications. Furthermore, flame stability within annular combustors is also better with respect to can-annular or other designs. This combustor is fuelled with either Jet-A or kerosene as previously mentioned. Fuel vapor is delivered into the combustor through 12 equally spaced (in the azimuthal direction) evaporation tubes placed inside the combustor itself. Ignition is achieved by a glow plug that is placed on the outer liner. Liner holes on the combustor liner, establish an airflow pattern within the liner that ensures easy light-up, efficient and stable combustion, adequate wall cooling and delivery of gases to the turbine with a suitable temperature profile.

Assembly of the reverse engineered micro turbojet engine is performed in CAD environment. Engine assembly view is provided in Figure 8.

Figure 1: Micro Turbojet Engine Used for This Study

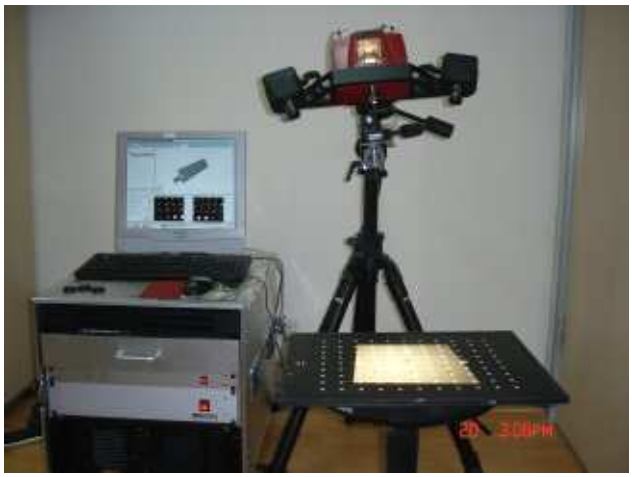

Figure 2: Optical Scanner

Figure 3: Turbine Rotor (Left-Point Cloud, Right-Solid)

TURBOJET CYCLE ANALYSIS

Cycle analysis is made assuming a real turbojet engine, nevertheless a number of simplifying assumptions are made [7]. For example air is assumed to be an ideal and calorifically perfect gas. Furthermore, engine is divided into two sections, namely; the cold section and the hot section.

The cold section starts at the inlet, ends at the combustion chamber entrance. Hot section encompasses the region from the combustion chamber inlet onwards in the streamwise direction. Certain parameters are kept constant in each region in order to simplify the analysis[8]. Representative values of the specific heats are chosen judiciously. These parameters are tabulated in Table 1.

The nomenclature recommended in the ARP.755 A (Aerospace Recommended Practice S.A.E.) has been followed where possible to point out the different stages of the engine. This station numbering is shown Fig. 9.

Calculations were performed assuming standart atmoshpheric conditions ($P_0 = 101.35\ kPa$,$T_0 = 298\ K$) at the engine inlet. Compressor polytropic efficiency is taken as $e_c = 0.8$, similarly turbine polytropic efficiency

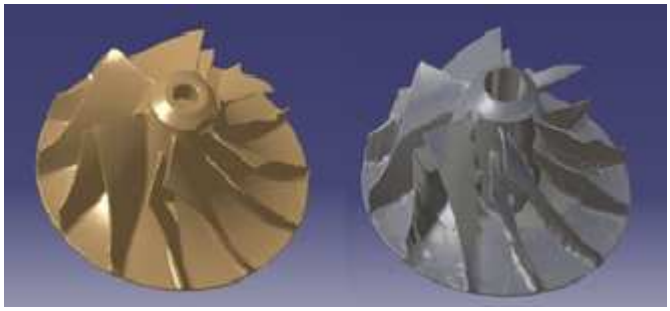

Figure 4: Impeller of the Centrifugal Compressor (Left-Point Cloud, Right-Solid)

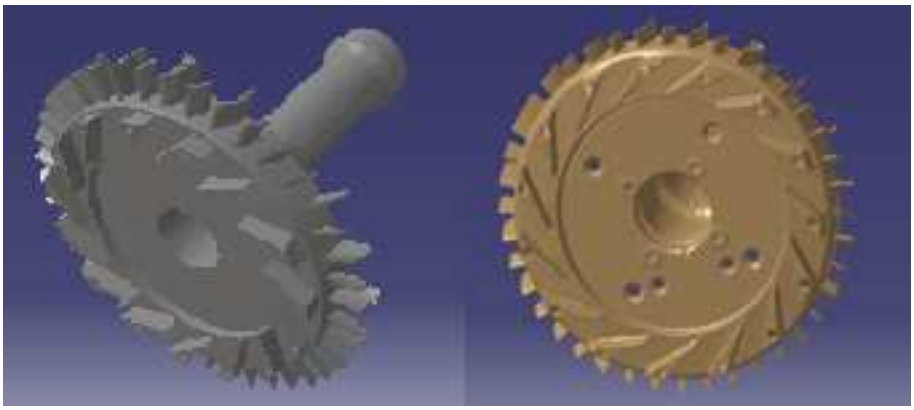

Figure 5: Compressor Diffuser (right-point cloud, left-solid)

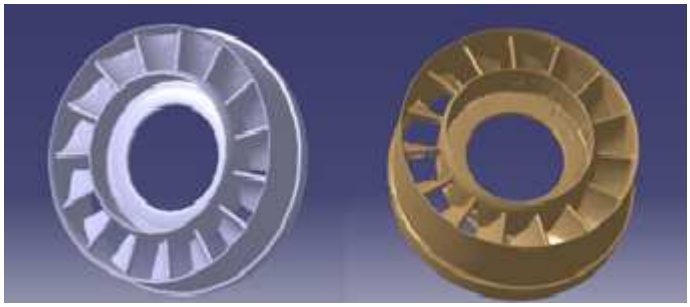

Figure 6: Turbine Inlet Guide Vane (right-point cloud, left-solid)

Table 1: Gas Parameter Variation Across the Engine

Parameter	Cold Section	Hot Section
Specific heats ratio	$\gamma_c = 1.4$	$\gamma_t = 1.3$
Heat capacity at constant pressure	$c_{p_c} = 1.004\ kJ/kgK$	$c_{p_t} = 1.239\ kJ/kgK$
Gas constant	$R_c = 0.287\ kJ/kgK$	$R_t = 0.286\ kJ/kgK$

is taken as $e_t = 0.7$. These choices are also consistent with the current technology level of micro turbojet engines.

Compressor pressure ratio is defined to be the total pressure ratio across the compressor and can also be related to total temperature ratio as per Eq. 1 [9].

$$\pi_c = \frac{P_{t3}}{P_{t1}} = [\frac{T_{t3}}{T_{t1}}]^{\frac{\gamma}{\gamma-1}} \tag{1}$$

Difference of total enthalpy across the compressor gives the power consumed by the centrifugal compressor per unit mass flow rate (Eq. 2).

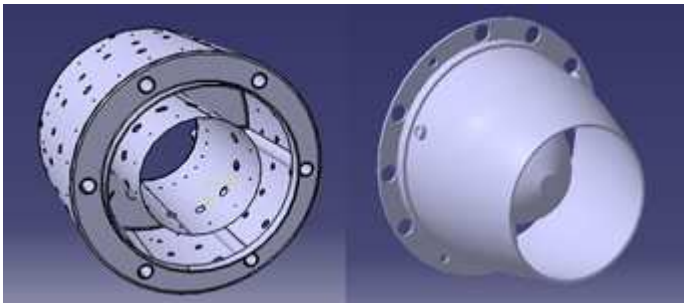

Figure 7: Left-Combustion Chamber, Right-Exhaust Nozzle

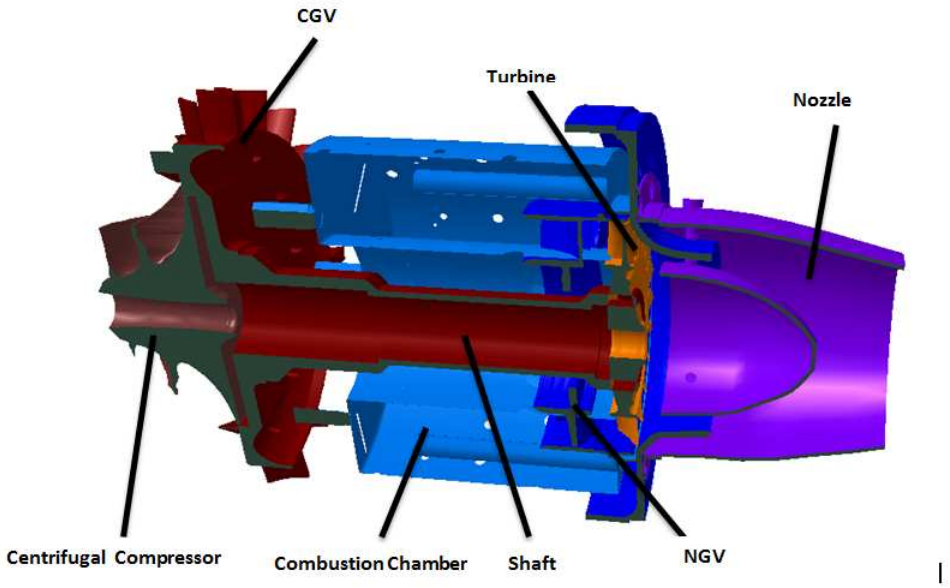

Figure 8: Assembly of the Simjet 2300-S-25 AES-GE Engine

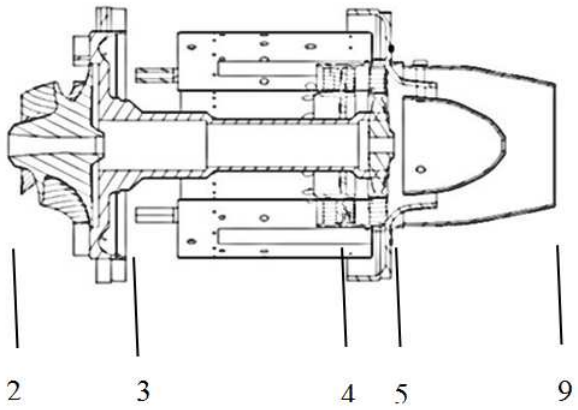

Figure 9: Station Numbering of the Engine (According to ARP.755A)

$$\dot{w}_c = h_{t3} - h_{t1} = c_{p_c}[T_{t3} - T_{t1}] = U_t v_2 \tag{2}$$

Tangential rotor velocity U_t can calculated in terms of mean blade radius r and angular velocity of rotor w (Eq. 3).

$$U_t = \omega r \tag{3}$$

The ratio of the exit swirl velocity to the rotor speed is called the slip factor ε (Eq. 4).

$$\varepsilon = \frac{v_2}{U_t} \tag{4}$$

Substitution of Eq. 4 into Eq. 3 provies an equation in terms of ε instead of v_2 (Eq. 5). Further arrangement yields Eq. 6.

$$T_{t3} - T_{t1} = \frac{{U_t}^2 \varepsilon}{c_{p_c}} \tag{5}$$

$$\pi_c = \frac{P_{t3}}{P_{t1}} = \left(1 + \frac{{U_t}^2 \varepsilon}{c_{p_c} T_{t1}}\right)^{\frac{\gamma_c}{\gamma - 1}} \tag{6}$$

The slip factor can be related to the number of vanes on the impeller. Number of vanes n and slip factor ε relation is given by Eq. 7 [8].

$$\varepsilon = 1 - \frac{2}{n} \tag{7}$$

Compressor pressure ratio depends on a single variable which is the rotor angular velocity ω. When its value increases so does the compression ratio up until the surge limit. The relationship between the rotor angular velocity and the compressor pressure ratio is shown in Figure 10.

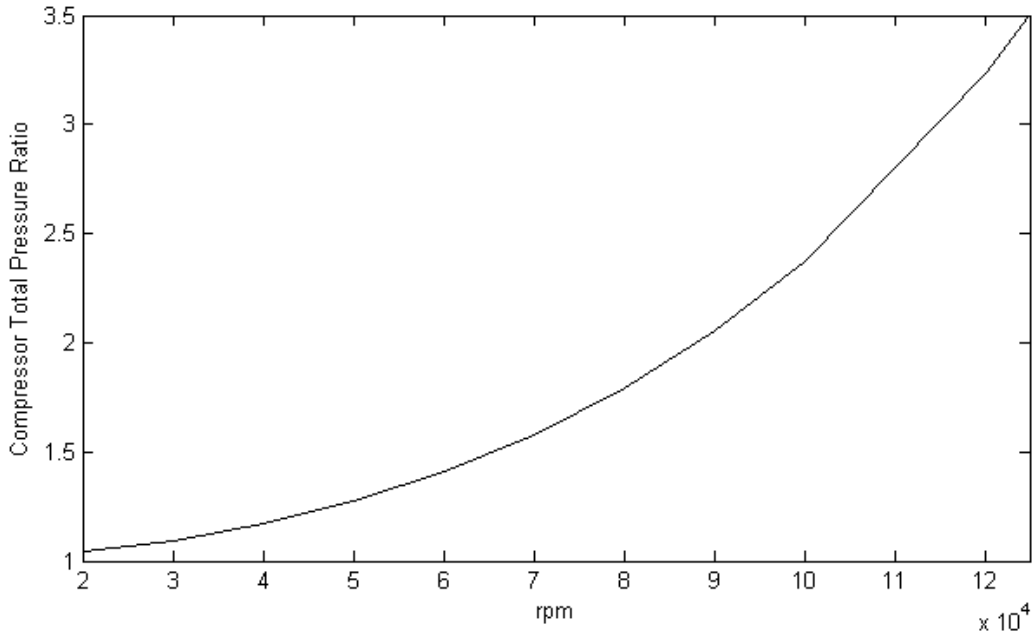

Figure 10: Compressor Total Pressure Ratio vs. Rotor Angular Velocity

Results of the cycle analysis are demonstrated such that the shaft speed is a parameter. Therefore, useful information can be obtained about the engine performance. Note that compression ratio can not be directly controlled by controller (i.e. the FADEC unit). Yet the rotor speed could indirectly be controlled by adjusting the fuel flow rate into the combustion chamber.

Sonic velocity at the freestream can easily be calculated (Eq. 8).

$$a_0 = \sqrt{\gamma_c R_c T_0} \tag{8}$$

Freestream velocity at the engine inlet is V_0 is related to the flight Mach number (Eq. 9)

$$V_0 = a_0 M_0 \tag{9}$$

Ratio of total to static values at the freestream are defined as recovery pressure and temperature ratios (Eq. 10- 11).

$$\tau_r = \frac{T_{t0}}{T_0} = 1 + \frac{1 + \gamma_c}{2} {M_0}^2 \tag{10}$$

$$\pi_r = \frac{P_{t0}}{P_0} = {\tau_r}^{\frac{\gamma_c}{\gamma_c - 1}} \tag{11}$$

Since flight is expected to be in the subsonic regime ($M_0 < 1$), diffuser pressure ratio and recovery efficiency can be taken as unity ($\eta_r = 1$,$\pi_d = 1$). Furthermore τ_λ is defined to be the ratio of the burner exit enthalpy to the ambient enthalpy for mathematical convenience (Eq. 12).

$$\tau_\lambda = \frac{h_{t_{be}}}{h_0} = \frac{c_{p_t} T_{t_4}}{c_{p_c} T_0} \tag{12}$$

For the rotating machinery components it is convenient to relate their temperature ratio to their pressure ratio by means of their efficiencies, which account for losses or real effectsite [6]. Therefore, compressor total temperature ratio can be ralated to total pressure ratio, if one has knowledge about polytropic efficiency (Eq. 13).

$$\tau_c = {\pi_c}^{\frac{\gamma_c - 1}{\gamma_c e_c}} \tag{13}$$

Compressor isentropic efficiency is provided by Eq. 14.

$$\eta_c = \frac{{\pi_c}^{\frac{\gamma_c - 1}{\gamma_c}} - 1}{\pi_c - 1} \tag{14}$$

Applying energy conservation principle to the combustor provides Eq. 15.

$$\dot{m}_0 c_{p_c} T_{t3} + \eta_b \dot{m}_f h_{PR} = \dot{m}_4 c_{p_t} T_{t4} \tag{15}$$

The fuel/air ratio f is the rate of fuel mass flow rate divided by the air mass flow rate (Eq. 16)

$$f = \frac{\dot{m}_f}{\dot{m}_0} \tag{16}$$

Manipulating the conservation of energy statement one can derive a relationship for the fuel/air ratio (Eq. 17).

$$f = \frac{\tau_\lambda - \tau_r \tau_c}{\eta_b h_{PR} / (c_{p_c} T_0) - \tau_\lambda} \tag{17}$$

For aeroengines the most limiting factor is temperature resistance of the materials. The most critical location is the turbine inlet (station 4). Consistent with the material limitations the turbine inlet temperature is chosen to be $T_{t4} = 1073\ K$. For this micro turbojet engine there is only one spool. Therefore, the power generated by the turbine drives the centrifugal compressor (Eq. 18). Note that, in order to account for mechanical losses (friction at the bearings etc.) η_m is chosen to be 0.98.

$$\dot{m}_0 c_{p_c} (T_{t3} T_{t2}) = \eta_m \dot{m}_4 c_{p_t} (T_{t4} T_{t5}) \tag{18}$$

Total temperature ratio across the turbine gives Eq. 19.

$$\tau_t = 1 - \frac{1}{\eta_m (1 + f)} \frac{\tau_r}{\tau_\lambda} (1 - \tau_t) \tag{19}$$

Similarly total pressure ratio across the turbine can be solved for using Eq. 20.

$$\pi_t = {\tau_t}^{\frac{\gamma_t}{(\gamma_t - 1) e_t}} \tag{20}$$

Compressor isentropic efficiency is calculated by Eq. 21.

$$\eta_c = \frac{1 - \pi_t}{1 - {\pi_t}^{\frac{1}{e_t}}} \tag{21}$$

Stagnation to static pressure ratio at exit of engine is calculated by Eq. 22.

$$\frac{P_{t9}}{P_9} = \left(1 + \frac{\gamma_t - 1}{2} {M_9}^2\right)^{\frac{\gamma_t}{\gamma_t - 1}} \tag{22}$$

For convenience Eq. 22 can be re-expressed in terms of component indices (Eq. 23)

$$\frac{P_{t9}}{P_9} = \frac{P_0}{P_9}\pi_r\pi_d\pi_c\pi_b\pi_t\pi_n \tag{23}$$

With the knowledge of stagnation to static pressure ratio then one can calculate the exit Mach number by Eq. 24.

$$M_9 = \sqrt{\frac{2}{\gamma_t - 1}\left(\frac{P_{t9}}{P_9}^{\frac{\gamma_t - 1}{\gamma_t}} - 1\right)} \tag{24}$$

Exhaust to freestream static temperature ratio can be expressed by Eq. 25.

$$\frac{T_9}{T_0} = \frac{\tau_\lambda \tau_t}{\left(\frac{P_{t9}}{P_9}\right)^{\frac{\gamma_t - 1}{\gamma_t}}} \tag{25}$$

Exhaust velocity to freestream Mach number ratio is also a key parameter for engine design[8]. It can be calculated by Eq. 26.

$$\frac{V_9}{a_0} = \sqrt{\frac{{a_9}^2 {M_9}^2}{{a_0}^2}} = M_9\sqrt{\frac{\gamma_t R_t T_9}{\gamma_c R_c T_0}} \tag{26}$$

Engine thrust can be obtained by applying the conservation of momentum principle to the engine control volume as in Eq. 27.

$$F = \dot{m}_9 V_9 - \dot{m}_0 V_0 + A_9(P_9 - P_0) \tag{27}$$

Dividing by the air mass flow rate and plugging in fuel/air ratio f into the equation, provides a relation for specific thrust (Eq. 28).

$$\frac{F}{\dot{m}_0} = a_0\left[(1+f)\frac{V_9}{a_0} - M_0 + (1+f)\frac{R_t(T_9/T_0)(1 - P_0/P_9)}{R_c(V_9/a_0)\gamma_c}\right] \tag{28}$$

One of the most important engine performance parameterws is the thrust specific fuel consumption. It is the ratio of fuel consumption to engine thrust [8](Eq. refeq:S). Note that, specific fuel consumption depends on flight conditions and throttle setting.

$$S = \frac{f}{F/\dot{m}_0} \tag{29}$$

The ratio of the rate of kinetic energy generation of the engine gas flow to the rate at which thermal energy is made available by the fuel is called the thermal efficiency of an aeroengine [8]. It can be calculated through Eq. 30.

$$\eta_T = \frac{{a_0}^2\left[(1+f)\left(\frac{V_9}{a_0}\right)^2 - {M_0}^2\right]}{2fh_{PR}} \tag{30}$$

By definition, propulsive efficiency is the ratio of thrust power to the rate of kinetic energy generation of the engine gas flow [8]. Propulsive efficiency can be calculated through Eq. 31.

$$\eta_P = \frac{2V_0\frac{F}{\dot{m}_0}}{{a_0}^2\left[(1+f)\left(\frac{V_9}{a_0}\right)^2 - {M_0}^2\right]} \tag{31}$$

Overall efficiency is the ratio of the thrust power to the rate at which thermal energy is made available by the fuel [8]. Overall efficiency can be obtained by combining of propulsive and thermal efficiencies (Eq. 32).

$$\eta_0 = \eta_P\eta_T \tag{32}$$

Performance calculation are carried out utilizing the above set of equations, for different shaft speeds and flight Mach numbers. Consequently, a set of engine characteristics are obtained. These are shown in Figures 11 through 16.

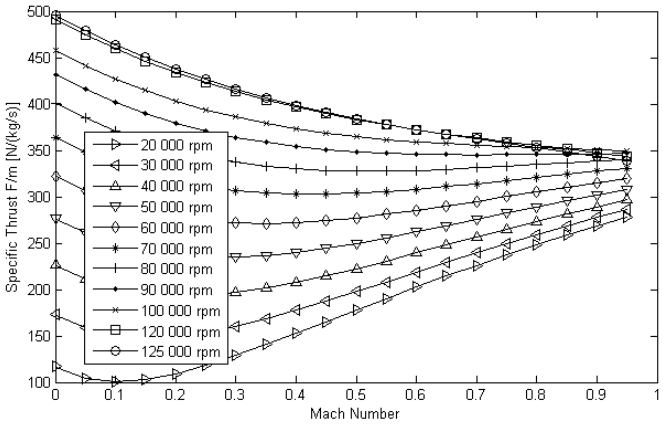

Figure 11: Specific Thrust versus Flight Mach Number

Figure 11 shows specific thrust as a function of flight Mach number, for a number of different shaft speeds ranging from 20k rpm to 130k rpm. Since the nominal shaft speed for this engine is 125k rpm it would be more practical to focus on that region in the plot.

Similarly fuel/air ratio is proportional to flight Mach number and angular rotor velocity (see Figure 12). This demonstrates that flying at the highest possible Mach number with the highest possible shaft speed is the most suitable condition for engine fuel economy. Figure 13 which shows specific fuel consumption as a function of flight Mach number confirms this as well.

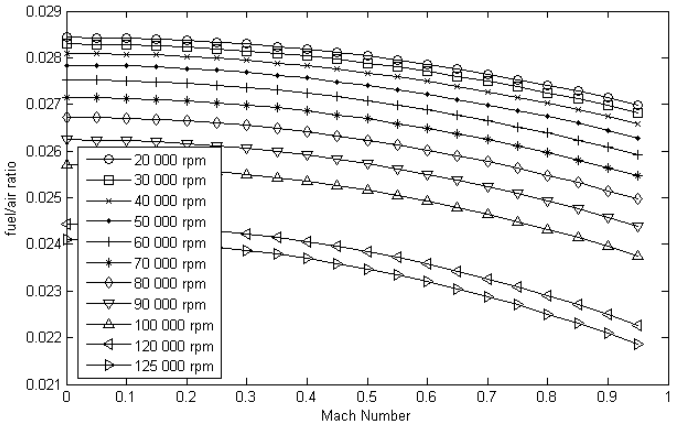

Figure 12: Fuel/Air Ratio versus Flight Mach Number

Thermal, propulsive and overall efficiencies of the micro turbojet engine at different operating conditions are provided in Figures 14 through 16.

Efficiency graphs show that the most efficient condition is obtained highest flight Mach number and shaft speed. However, also note that both flight Mach number and shaft speed have constraints due to structural and aerodynamic limits.

A two dimensional cascade view of the turbine stage is illustrated in Figure 17. Relative and absolute flow angles and flow speeds are calculated via velocity triangles. These velocity triangles and corresponding nomenclature are conviniently providedin Figure 18.

Engine performance parameters at the nominal operating condition are summarized in Table 3. Note that the nominal shaft speed is 125k rpm and flight Mach number is 0.75 for this aeroengine.

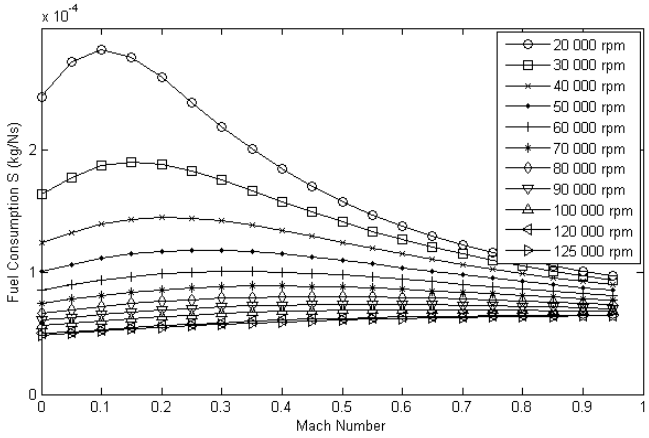

Figure 13: Flight Mach Number versus Specific Fuel Consumption

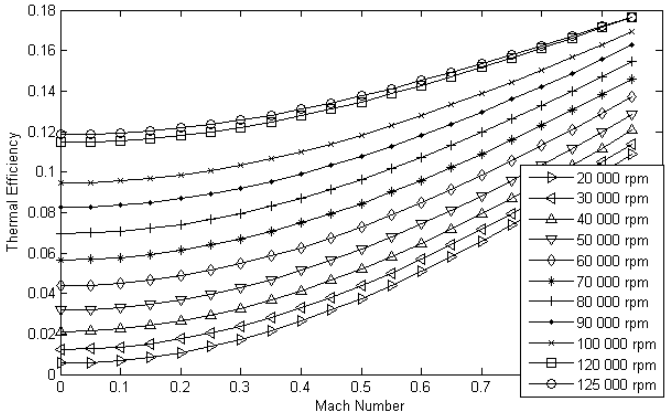

Figure 14: Thermal Efficiency versus Flight Mach Number

Table 2: Turbine Stage Parameters

Parameter	Value
T_{t4}	1073 K
$T_{4.5}$	931 K
U	361 m/s
c_1	592 m/s
α_1	0°
c_2	827 m/s
W_2	630 m/s
β_2	20°
W_{2u}	215 m/s
V_2	827m/s
u	592m/s

Table 3: Engine Performance Parameters

Parameter	Calculated Values	Manufacturer Values
Air Flow Rate	0.314 kg/s	0.294 kg/s
Thrust	112.36 N	111.2 N
Fuel Consumption	0.514 l/min	0.354 l/min

CONCLUSION

Micro turbojet engines are used as propulsion systems for mini UAVs, target drones, cruise missiles etc. They are

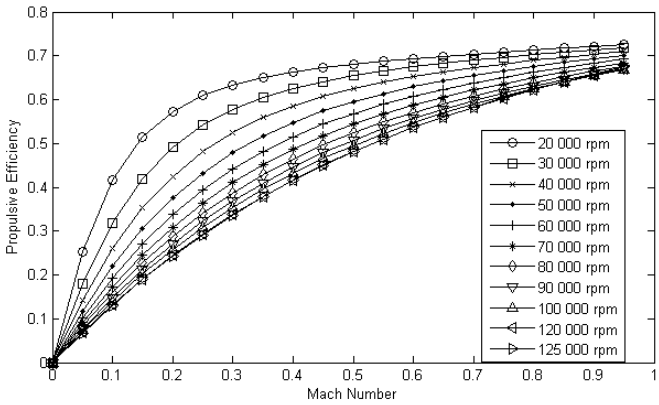

Figure 15: Propulsive Efficiency versus Flight Mach Number

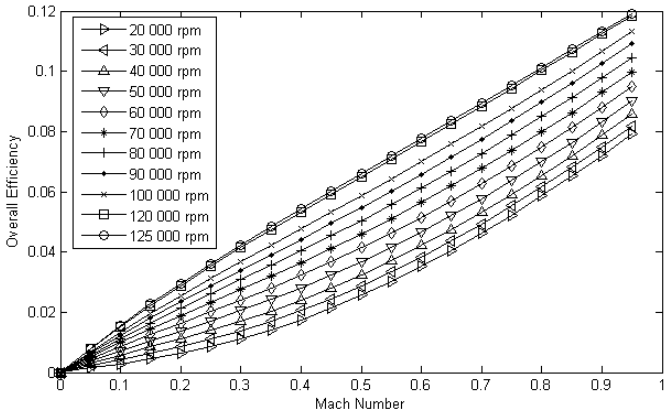

Figure 16: Overall Efficiency versus Flight Mach Number

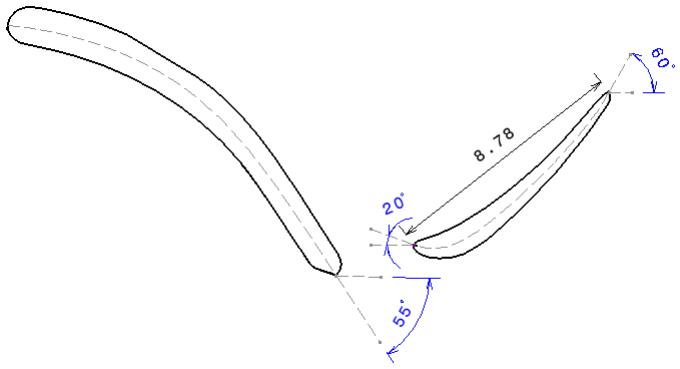

Figure 17: Blade Geometries for the Turbine Stage

also commonly used for educational purposes in thermodynamics related courses. In this paper such an engine is designed not from scratch but rather utilizing reverse engineering techniques. First, its geometric features are recovered on a part by part basis, they are also assembled in the CAD environemnt. Second, a performance study is carried out analytically based on the geometry of the engine. Variation of engine performance due to certain parameters of interest are investigated. Note that, performance parameters that are calculated analytically are indeed close to manufacturer specifications. This can be taken as a benchmark regarding the level of success of this study. Furthermore, this engine can serve as a baseline model for prospective more advanced micro turbojet engines. This paper also demonstrates the use of reverse engineering practices. Reverse engineering can reduce to overall design time especially when there is a technology gap. After this

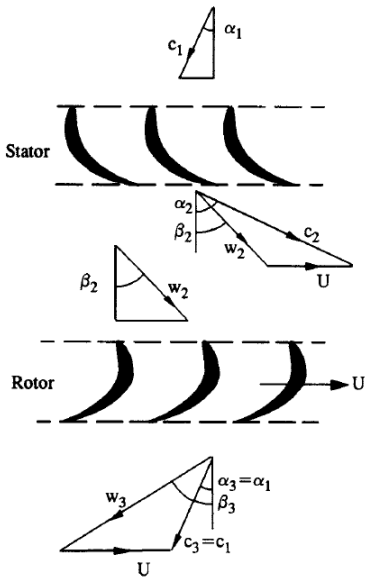

Figure 18: Velocity Triangles for the Turbine Stage

gap is closed, then one can proceed with conventional design practices.

ACKNOWLEDGEMENT

We would like to gratefully acknowledge some quite fruitful discussions with Mr.Sait Ziya Aksoy during the Aeroengine Design Course at ITU.

References

[1] C. Rodgers, "Turbofan design options for mini UAV's," in *37th AIAA/ASME/SAE/ASEE Joint Propulsion Conference and Exhibit*, 2001.

[2] P.Akbari and N.Muller, "Performance investigation of small gas turbine engines topped with wave rotors," in *39th AIAA/ASME/SAE/ASEE Joint Propulsion Conference and Exhibit*, 2003.

[3] D. Akca, A. Grun, B. Breuckmann, and C. Lahanier, "High definition 3D scanning of art objects and paintings," *Optical 3D Measurement Techniques VIII*, 2007.

[4] S.L. Dixon and C.A. Hall, *Fluid Mechanics and Thermodynamics of Turbomachinery*, Butterworth-Heinemann, 2010.

[5] A. Ceylanoglu, "An accelerated aerodynamic optimization approach for a small turbojet engine centrifugal compressor," M.S. thesis, Middle East Technical University, 2009.

[6] Wiliam W. Bathie, *Fundamentals of Gas Turbines*, Wiley, second edition, 1996.

[7] I.R. Lewis, *Turbomachinery Performance Analysis*, John Wiley and Sons, 1996.

[8] J. D. Mattingly, W. Heiser, and D. Pratt, *Aircraft Engine Design*, AIAA Education Series. AIAA, second edition, August 2006.

[9] J. D. Mattingly and H. von Ohain, *Elements of Propulsion: Gas Turbines and Rockets*, AIAA Education Series. AIAA, August 2006.